SCIENTIFIC REPORTS

Tunable mid-infrared coherent perfect absorption in a graphene meta-surface

Yuancheng Fan[1], Zhe Liu[2], Fuli Zhang[1], Qian Zhao[3], Zeyong Wei[4], Quanhong Fu[1], Junjie Li[2], Changzhi Gu[2] & Hongqiang Li[4]

Graphene has drawn considerable attention due to its intriguing properties in photonics and optoelectronics. However, its interaction with light is normally rather weak. Meta-surfaces, artificial structures with single planar function-layers, have demonstrated exotic performances in boosting light-matter interactions, e.g., for absorption enhancement. Graphene based high efficiency absorber is desirable for its potential applications in optical detections and signal modulations. Here we exploit graphene nanoribbons based meta-surface to realize coherent perfect absorption (CPA) in the mid-infrared regime. It was shown that quasi-CPA frequencies, at which CPA can be demonstrated with proper phase modulations, exist for the grapheme meta-surface with strong resonant behaviors. The CPA can be tuned substantially by merging the geometric design of the meta-surface and the electrical tunability of graphene. Furthermore, we found that the graphene nanoribbon meta-surface based CPA is realizable with experimentally achievable graphene sample.

Recently, graphene is been widely investigated for potential applications in photonics and optoelectronics[1–5]. It exhibits much stronger binding of surface plasmon polaritons[6], and the Dirac fermions provides ultrawideband tunability through electrostatic field, magnetic field or chemical doping[7,8]. One key feature of graphene is that it is almost transparent to optical waves[9] due to the relatively low carrier concentrations in a monolayer atomic sheet. Boosting the light-matter interaction in graphene is one important issue to address to take further advantage of graphene in optoelectronic devices. For example, to realize functionality like optical insulator[10] similar to gapped graphene[11,12] for nanoelectronics, which is essential for myriad applications in all-optical systems and components of much miniaturized optical circuits[13,14].

Artificially engineered photonic structures have been employed as a platform for boosting light-matter interactions for decades[15,16]. Optical absorption enhancement had been demonstrated in a photonic crystal nanocavity for high-contrast electrooptic modulation[17]. In the meanwhile, metamaterials[18,19] with even miniaturized elements are promising for the manipulation of light in a subwavelength scale. Especially the metamaterials with a single planar function-layer, or meta-surface[20,21], has been intensively studied in recent years for various possibilities to manipulate light peculiarly[22–26]. The meta-surface has also found its close connection to graphene: replacing metals with graphene makes the meta-surface even miniaturized for frequency-agile responses[27]; and the light-graphene interactions can be significantly modified in an atomically thin graphene meta-surface in return. It was reported that optical absorption enhancement can be achieved in periodically doped graphene nanodisks, in which periodic graphene nanodisks are overlying on a substrate or on a dielectric film coating on metal, the excitation of electric

[1]Key Laboratory of Space Applied Physics and Chemistry, Ministry of Education and Department of Applied Physics, School of Science, Northwestern Polytechnical University, Xi'an 710129, China. [2]Beijing National Laboratory for Condensed Matter Physics, Institute of Physics, Chinese Academy of Sciences, Beijing 100190, China. [3]State Key Laboratory of Tribology, Department of Mechanical Engineering, Tsinghua University, Beijing 100084, China. [4]Key Laboratory of Advanced Micro-structure Materials (MOE) and School of Physics Science and Engineering, Tongji University, Shanghai 200092, China. Correspondence and requests for materials should be addressed to Y.F. (email: phyfan@nwpu.edu.cn)
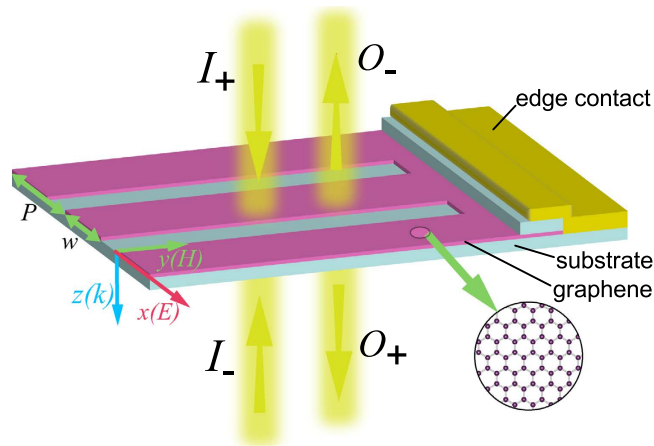
Figure 1. Schematic of a graphene ribbon meta-surface illustrated by two counter-propagating and coherently modulated input beams (I_+ and I_-, the electric polarization is along *x*-axis, and propagate along $\pm z$-directions), O_+ and O_- represent the amplitudes of output beams.

mode of the nanodisks together with multi-reflection from the assistants of total internal reflection and metal reflection can result in a complete optical absorption[28]. Graphene micro/nanoribbons, ring resonators, mantles, nano-crosses and super-lattices have also been attempted for manipulating the terahertz/infrared waves[29–41]. A comparative study[37] found that the fundamental electric dipolar mode provides stronger light-graphene interaction at terahertz frequencies than the magnetic and higher-order electric modes, it is also found that the maximum absorption in a monolayer graphene is 50%, which is associated with a real number effective surface conductivity $2/\eta_0$ where η_0 represents the characteristic impedance of vacuum[42]. The concept of coherent perfect absorption in structured systems[43–52] was introduced into a suspending monolayer graphene for 100% absorption of terahertz waves[53]. However, the proposed non-resonant CPA based on the intrinsic Drude response of graphene is realizable only in the few-terahertz range with achievable graphene samples.

In this paper, we propose a tunable mid-infrared coherent perfect absorber with a graphene nanoribbon based meta-surface. It is found that quasi-CPA frequencies, which is the necessary formation condition of coherent absorption, does exist in the mid-infrared regime for properly designed graphene nanoribbon arrays. The scattering of coherent beams can be perfectly suppressed at the quasi-CPA frequencies with proper phase modulations on the input beams. For the case with two crosses on the transmission and reflection spectra, we can achieve coherent perfect absorption at the two quasi-CPA frequencies, simultaneously. The flexible tunabilities of the graphene meta-surface based CPA are of interests for tunable infrared detections and signal modulations.

Results and Discussion

Figure 1 shows the schematic of the proposed graphene nanoribbons based meta-surface and corresponding excitation configuration with two counter-propagating and coherently modulated optical beams (I_+ and I_-), O_+ and O_- are the respective output magnitudes, the graphene sheet is illuminated with perpendicularly polarized light (electric vector E is parallel to the *x*-axis). The meta-atoms, i.e., graphene nanoribbons, are periodically arranged in *x-y* plane with the lattice (along *x* axis) constant and ribbon's width being P and w, respectively. Both lattice constant and width of the graphene nanoribbon meta-atoms play important roles in determining the optical resonant behaviors of graphene meta-surface, the lattice constant is set to be $P = 0.7\,\mu$m for the study of CPA in the mid-infrared regime.

The graphene layer is considered as a sheet material modeled with complex surface conductivity (σ_g) since a one-atom-thick graphene sheet is sufficiently thin compared with the concerned wavelength. In the theoretical perspective based on random-phase-approximation (RPA)[54–56], the complex conductivity of graphene can be described by the Drude model as $\sigma_g = ie^2E_F/\pi\hbar^2(\omega + i\tau^{-1})$, especially in heavily doped region and low frequencies (far below Fermi energy), where E_F represents the Fermi energy, $\tau = \mu E_F/ev_F^2$ is the relaxation rate with the mobility $\mu = 10^4\,$cm^{2}V^{-1}s^{-1} and Fermi velocity $v_F \approx 10^6\,$m/s.

We first took $E_F = 0.5\,$eV. Figure 2a presents the spectra of the reflection coefficients (r) and transmission coefficients (t) for the case of graphene nanoribbon meta-surface with width of $w = 0.33\,\mu$m. We can see an obvious resonance around 23.0 THz. The resonance was confirmed to be electric dipolar mode (which will be verified from the effective surface conductivity below), similar to the low-frequency resonance of split-ring-resonators as that in[37]. The excitation of electric dipolar mode leads to the enhancement of absorption in the graphene sheet, however, the maximum limit is 50%.
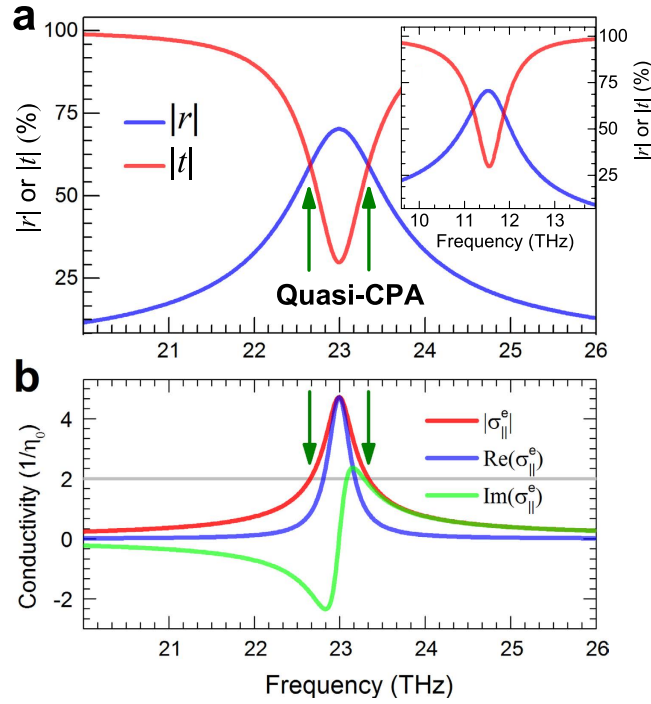
Figure 2. (**a**) Spectra of the reflection and transmission coefficients of a graphene nanoribbon meta-surface ($w = 0.33\,\mu$m), the quasi-CPA points at the crosses of the scattering spectra are indicated with arrows. (**b**) Absolute values, real and imaginary parts of the effective surface conductivities of the corresponding graphene nanoribbon meta-surface.

The complex scattering coefficients ($O_\pm$) of the graphene nanoribbon meta-surface can be related to the two input beams ($I_\pm$, and in this paper the two input beams are set to be of equal amplitude I) through a scattering matrix, S_g, defined as:

$$\begin{pmatrix} O_+ \\ O_- \end{pmatrix} = S_g \begin{pmatrix} I_+ \\ I_- \end{pmatrix} = \begin{pmatrix} t_+ & r_- \\ r_+ & t_- \end{pmatrix} \begin{pmatrix} Ie^{i\varphi_+} \\ Ie^{i\varphi_-} \end{pmatrix},$$

(1)

where $(t/r)_+$ and $(t/r)_-$ are scattering elements of forward (irradiate towards z_+, I_+) and backward (irradiate towards z_-, I_-) beams, since the linear monolayer graphene under investigation is of reciprocity and spatial symmetry, the scattering matrix can be simplified with $t_\pm = t$ and $r_\pm = r$. Then the amplitude of the scattering coefficients would be

$$|O_+| = |O_-| = |tIe^{i\varphi_+} + rIe^{i\varphi_-}|.$$

(2)

The scatterings of the input beams are required to be inhibited to demonstrate a CPA, that is $tIe^{i\phi_+} = -rIe^{i\phi_-}$, from which we can get the necessary condition for CPA performance: $|t| = |r|$.

Since the high-order scatterings of the deep-subwavelength graphene nanoribbons are negligible, the graphene meta-surface can be formalized with effective surface conductivities $\left(\sigma_\parallel^e\right)$ and its scattering coefficients of normal incident light can be got with a transfer matrix formalism:

$$t_\perp = \frac{2}{2 + \sigma_\parallel^e \eta_0},$$

(3)

$$r_\perp = \frac{\sigma_\parallel^e \eta_0}{2 + \sigma_\parallel^e \eta_0},$$

(4)

where η_0 is the wave impedance of free space.

It can be seen from Fig. 2a there exists two frequencies (22.65 THz, and 23.33 THz), which we call *quasi-CPA* point, where $|t| = |r|$ implies the necessary condition for suppressing the scattering fields to completely absorb coherent input beams of equal-intensity. In the view of experiments, graphene generally needs to be transferred onto some substrate, we studied the scattering responses of a nanoribbon array [with same geometry as that in Fig. 2a] sandwiched in between two 45 nm-thick hexagonal boron nitride

3
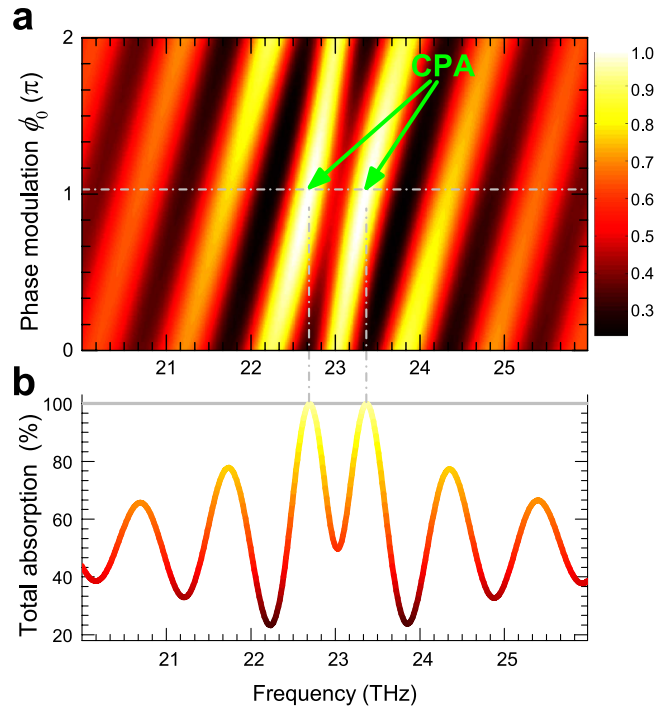
Figure 3. A two-dimensional false-color plot of the normalized total absorptions as a function of frequency and phase modulation ϕ_0, the exact CPA points are denoted with green arrows.
(**b**) Normalized total absorption as a function of frequency for the phase modulation $\phi_0 = 1.03\pi$.

(h-BN) substrates, which was suggested as an exceptionally clean environment for achieving high confinement and low levels of plasmon damping in graphene[57] and is suitable for the one-dimensional high-quality electrical contact[58] (see the illustration in Fig. 1). The dielectric function of which was taken from experimental studies[57,59]. As can be seen from the inset of Fig. 2a, the resonant frequency shifts to lower frequency as expected because of the introduction of the substrate, and there keeps two quasi-CPA frequencies. For simplicity and without loss of generality, we will consider free-standing graphene meta-surfaces.

From Eq. (3), we can also get the formation condition for CPA in an effective medium scheme as: $\left| \sigma_{\parallel}^{e} \right| \eta_0 = 2$. To verify this, we used a recently proposed sheet retrieval method[60] to extract the effective surface conductivity $\sigma_{\parallel}^{e}$ of the graphene nanoribbon meta-surface. Figure 2(b) shows the absolute, real and imaginary parts of the effective surface conductivities corresponding to Fig. 2a, It is obvious that there is a Lorentz-resonance around 23.0 THz on the effective electric conductivity spectrum, which confirms the excitation of electric dipolar mode. The extracted magnetic conductivity does not show any resonant feature around this electric resonance, so we have not included the corresponding result here. And it is also seen that the condition $\left| \sigma_{\parallel}^{e} \right| \eta_0 = 2$ is fulfilled at the two quasi-CPA frequencies, which indicate the validity of describing the graphene nanoribbon meta-surface with the effective surface conductivity.

To implement the perfect absorption with the graphene meta-surface, we set a chirped phase modulation $\Delta \phi (f) = \phi_+ - \phi_- = \phi_0 + kf$ on the beams $I_{\pm}$, with f being the frequency, and $k = -1.87 \times 10^{-12} \pi$ being the chirped factor to compensate the frequency dispersion. The plotted false-color map of the normalized spectra of total absorptions in Fig. 3a, shows the detailed dependence on ϕ_0. We see that a proper phase modulation ($\phi_0 = 1.03\pi$) of the input coherent beams leads to significant suppression of the scattering outputs at the quasi-CPA frequencies. The normalized total absorption as a function of frequency for the phase modulation $\phi_0 = 1.03\pi$ is plotted in Fig. 3b. We can see total absorption at both the two quasi-CPA frequencies. The significant boosting of the absorption implies destructive interference which prevents the coherent beams from escaping the absorbing channel of the graphene meta-surface, demonstrating completely absorption of the coherent input beams.

The meta-surface structures together with the electrically-controlled graphene will provide more wider tunable space for the design of mid-infrared CPA, we first consider the geometric tunability of the graphene nanoribbon based CPA. Figure 4 shows the dependence of the difference $(|r| - |t|)$ of the scattering coefficients (r and t) of the graphene meta-surface on the widths of nanoribbons. We can see that the resonant frequency of the electric dipolar mode shows a monotonous red-shift with the increase of w, which is similar the cut-wire case[42] (actually, the ribbon structure is the special situation of cut-wire with graphene covers all the lattice range along x axis. Increasing of the width w or the graphene' filling factor in the unit cell of the meta-surface leads to stronger light-graphene interaction, i.e. high resonant
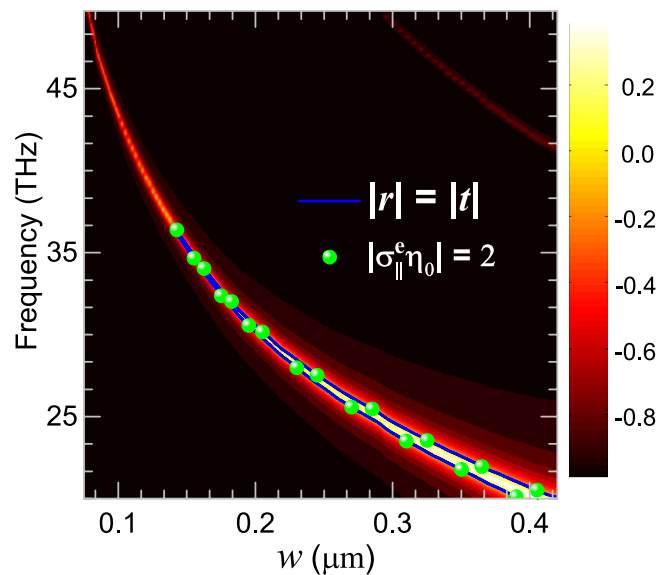
Figure 4. Geometric tunability of the graphene meta-surface CPA: Spectra of the difference ($|r|-|t|$) of the scattering coefficients (r and t) for the graphene meta-surface width increasing from 0.075 μm to 0.42 μm. The solid line indicates quasi-CPA points where $|r| = |t|$, while the spheres represent the extracted surface conductivities with values $\left|\sigma_{\parallel}^{e}\right|\eta_0 = 2$.
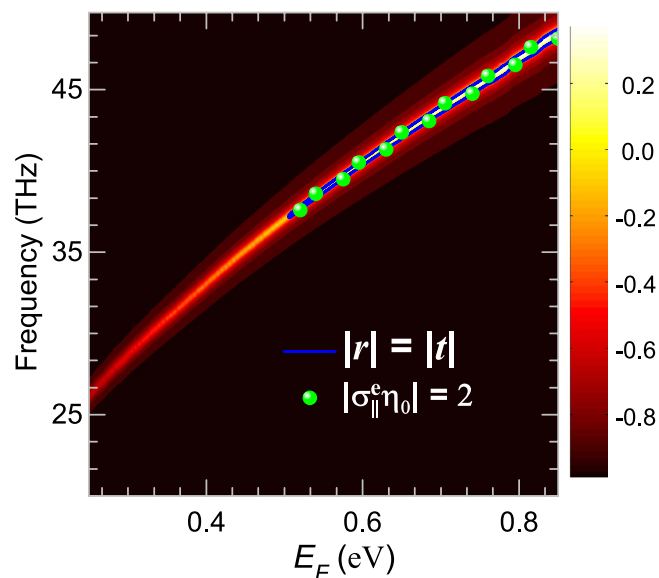
Figure 5. Electric tunability of the graphene meta-surface CPA: Spectra of the difference ($|r|-|t|$) of the scattering coefficients (r and t) for the graphene meta-surface with Fermi energy E_F ranging from 0.25 eV to 0.85 eV. The solid line indicates quasi-CPA points where $|r| = |t|$, while the spheres represent the extracted surface conductivities with values $\left|\sigma_{\parallel}^{e}\right|\eta_0 = 2$.

strength of the electric dipolar resonance, and thus higher r and lower t around the resonance that introduce a regime where $|r| - |t| \geq 0$ starting from $w = 0.138 \,\mu$m, which has its boundary (as the solid line indicated) being the quasi-CPA points. The discrete spheres on top of the solid curve, representing the extracted surface conductivities with $\left|\sigma_{\parallel}^{e}\right|\eta_0 = 2$, also imply the formation condition of CPA is fulfilled at the boundary. At these quasi-CPA points, we can completely suppress the scatterings of the graphene meta-furface with proper phase modulations as that showed in Fig. 3.

On the other hand, the graphene meta-surface is also expected to have higher resonant strength for graphene with larger Fermi level[3,42]. The dependence on Fermi energy of the difference ($|r| - |t|$) of the scattering coefficients are plotted in Fig. 5 [the width of the graphene nanoribbon was set to be 0.138 μm,
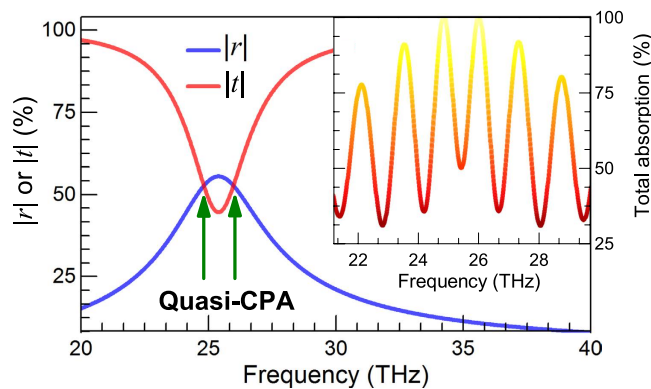
Figure 6. Scattering coefficients of a graphene nanoribbon array with experimental data (Yan *et al.* data), the inset shows normalized total absorption for proper phase modulation.

the left edge of the solid boundary in Fig. 4], it can be seen that the resonant frequency shifts to higher frequencies and the resonant strength becomes higher while the Fermi level changes from to 0.25 eV to 0.85 eV. Similar to the influence of the width of nanoribbons, the light-graphene interaction is enhanced for better resonant behaviors, and thus a regime starting from 0.5 eV where $|r| - |t| \geq 0$ with its boundary being the quasi-CPA frequencies. Combining the two functional bands for CPA, we see that it is freely to achieve CPA at desired frequency in an ultra-wide range by merging the geometric and electrical tunabilities. And the discrete spheres representing the extracted surface conductivities in Fig. 5 again confirm that $\left| \sigma_\parallel^e \right| \eta_0 = 2$ is equivalent to the quasi-CPA condition $|r| = |t|$ for graphene nanoribbons based meta-surface.

Here, we also consider a graphene nanoribbon array ($P = 0.22\,\mu$m, $w = 0.20\,\mu$m) made from experimentally practical graphene, i.e., the Yan *et al.* graphene with Drude weight $e^2 E_F / \pi \hbar^2 = 76.0$ GHz/Ω and collision frequency $\tau^{-1} = 9.8$ THz[2,5]. The spectra of the scattering coefficients are presented in Fig. 6a, from which, a electric resonance is found around 25.5 THz with two associate quasi-CPA frequencies. The inset shows perfect absorption can be achieved at these two quasi-CPA frequencies with proper phase modulation. This suggest that the graphene nanoribbon meta-surface based CPA is feasible with high-quality Chemical Vapour Deposition (CVD) grown graphene samples.

Conclusions

In conclusion, we show that graphene nanoribbons based meta-surface can be employed for perfectly suppressing scattering of mid-infrared radiations for CPA. And the quasi-CPA frequency can be found from the effective surface conductivity spectra where $\left| \sigma_\parallel^e \right| \eta_0 = 2$. Furthermore, the CPA can be tuned in a ultra-wide frequency band by considering both the geometric tunability and electrically-controlled charge-carrier density in graphene. We expect potential applications of coherent modulations in optical detections and signal processing with structured two-dimensional materials.

Methods

The numerical calculation results were obtained with a finite-integration-technique based electromagnetic solver (CST Microwave Studio). The periodic boundary conditions were set for the simulation of periodic graphene nanoribbon structures. The effective surface conductivities of the graphene nanoribbon based meta-surfaces were carried out using a recently proposed sheet retrieval method[60].

References

1. Bonaccorso, F., Sun, Z., Hasan, T. & Ferrari, A. C. Graphene photonics and optoelectronics. *Nat. Photonics* **4,** 611–622 (2010).
2. Yan, H. *et al.* Tunable infrared plasmonic devices using graphene/insulator stacks. *Nat. Nanotechnol* **7,** 330–334 (2012).
3. García de Abajo, F. J. Graphene plasmonics: Challenges and opportunities. *ACS Photonics* **1,** 135–152 (2014).
4. Low, T. & Avouris, P. Graphene plasmonics for terahertz to mid-infrared applications. *ACS Nano* **8,** 1086–1101 (2014).
5. Tassin, P., Koschny, T. & Soukoulis, C. M. Graphene for terahertz applications. *Science* **341,** 620–621 (2013).
6. Jablan, M., Buljan, H. & Soljačić, M. Plasmonics in graphene at infrared frequencies. *Phys. Rev. B* **80,** 245435 (2009).
7. Koppens, F. H. L., Chang, D. E. & García de Abajo, F. J. Graphene plasmonics: A platform for strong light–matter interactions. *Nano Lett.* **11,** 3370–3377 (2011).
8. Vakil, A. & Engheta, N. Transformation optics using graphene. *Science* **332,** 1291–1294 (2011).
9. Nair, R. R. *et al.* Fine structure constant defines visual transparency of graphene. *Science* **320,** 1308 (2008).
10. Yablonovitch, E. Photonic crystals: semiconductors of light. *Sci. Am.* **285,** 47–51, 54 (2001).
11. Yao, Y., Ye, F., Qi, X.-L., Zhang, S.-C. & Fang, Z. Spin-orbit gap of graphene: First-principles calculations. *Phys. Rev. B* **75,** 041401 (2007).
12. Zhang, Z. *et al.* Extend the omnidirectional electronic gap of thue-morse aperiodic gapped graphene superlattices. *Appl. Phys. Lett.* **101,** 252104 (2012).

13. Engheta, N. Circuits with light at nanoscales: Optical nanocircuits inspired by metamaterials. *Science* **317,** 1698–1702 (2007).
14. Fan, Y. *et al.* Subwavelength electromagnetic diode: One-way response of cascadinig nonlinear meta-atoms. *Appl.Phys. Lett.* **98,** 151903 (2011).
15. Hess, O. *et al.* Active nanoplasmonic metamaterials. *Nat. Mater.* **11,** 573–584 (2012).
16. Kauranen, M. & Zayats, A. V. Nonlinear plasmonics. *Nat. Photonics* **6,** 737–748 (2012).
17. Gan, X. *et al.* High-contrast electrooptic modulation of a photonic crystal nanocavity by electrical gating of graphene. *Nano Lett.* **13,** 691–696 (2013).
18. Smith, D. R., Pendry, J. B. & Wiltshire, M. C. K. Metamaterials and negative refractive index. *Science* **305,** 788–792 (2004).
19. Soukoulis, C. M. & Wegener, M. Past achievements and future challenges in the development of three-dimensional photonic metamaterials. *Nat. Photonics* **5,** 523–530 (2011).
20. Kildishev, A. V., Boltasseva, A. & Shalaev, V. M. Planar photonics with metasurfaces. *Science* **339,** 6125 (2013).
21. Yu, N. & Capasso, F. Flat optics with designer metasurfaces. *Nat. Mater* **13,** 139–150 (2014).
22. Yu, N. *et al.* Light propagation with phase discontinuities: Generalized laws of reflection and refraction. *Science* **334,** 333–337 (2011).
23. Ni, X., Emani, N. K., Kildishev, A. V., Boltasseva, A. & Shalaev, V. M. Broadband light bending with plasmonic nanoantennas. *Science* **335,** 427 (2012).
24. Sun, S. *et al.* Gradient-index meta-surfaces as a bridge linking propagating waves and surface waves. *Nat. Mater.* **11,** 426–431 (2012).
25. Yin, X., Ye, Z., Rho, J., Wang, Y. & Zhang, X. Photonic spin hall effect at metasurfaces. *Science* **339,** 1405–1407 (2013).
26. Shitrit, N. *et al.* Spin-optical metamaterial route to spin-controlled photonics. *Science* **340,** 724–726 (2013).
27. Chen, H.-T. *et al.* Experimental demonstration of frequency-agile terahertz metamaterials. *Nat. Photonics* **2,** 295–298 (2008).
28. Thongrattanasiri, S., Koppens, F. H. L. & García de Abajo, F. J. Complete optical absorption in periodically patterned graphene. *Phys. Rev. Lett.* **108,** 047401 (2012).
29. Ju, L. *et al.* Graphene plasmonics for tunable terahertz metamaterials. *Nat. Nanotechnol.* **6,** 630–634 (2011).
30. Alaee, R., Farhat, M., Rockstuhl, C. & Lederer, F. A perfect absorber made of a graphene micro-ribbon metamaterial. *Opt. Express* **20,** 28017–28024 (2012).
31. He, S., Zhang, X. & He, Y. Graphene nano-ribbon waveguides of record-small mode area and ultra-high effective refractive indices for future vlsi. *Opt. Express* **21,** 30664–30673 (2013).
32. Yan, H. *et al.* Damping pathways of mid-infrared plasmons in graphene nanostructures. *Nat. Photonics* **7,** 394–399 (2013).
33. Zhang, Y., Feng, Y., Zhu, B., Zhao, J. & Jiang, T. Graphene based tunable metamaterial absorber and polarization modulation in terahertz frequency. *Opt. Express* **22,** 22743–22752 (2014).
34. Liu, P., Cai, W., Wang, L., Zhang, X. & Xu, J. Tunable terahertz optical antennas based on graphene ring structures. *Appl. Phys. Lett.* **100,** 153111 (2012).
35. Wang, W. Plasmons and optical excitations in graphene rings. *J. Phys.: Condens. Matter* **24,** 402202 (2012).
36. Papasimakis, N., Thongrattanasiri, S., Zheludev, N. I. & García de Abajo, F. J. The magnetic response of grapheme split-ring metamaterials. *Light: Sci. Appl* **2,** e78 (2013).
37. Fan, Y., Wei, Z., Zhang, Z. & Li, H. Enhancing infrared extinction and absorption in a monolayer graphene sheet by harvesting the electric dipolar mode of split ring resonators. *Opt. Lett.* **38,** 5410–5413 (2013).
38. Chen, P.-Y. & Alù, A. Atomically thin surface cloak using graphene monolayers. *ACS Nano* **5,** 5855–5863 (2011).
39. Cheng, H. *et al.* Mid-infrared tunable optical polarization converter composed of asymmetric graphene nanocrosses. *Opt. Lett.* **38,** 1567–1569 (2013).
40. Fan, Y., Wei, Z., Li, H., Chen, H. & Soukoulis, C. M. Photonic band gap of a graphene-embedded quarter-wave stack. *Phys. Rev. B* **88,** 241403(R) (2013).
41. Zhu, W., Xiao, F., Kang, M., Sikdar, D. & Premaratne, M. Tunable terahertz left-handed metamaterial based on multilayer graphene-dielectric composite. *Appl. Phys. Lett.* **104,** 051902 (2014).
42. Fan, Y., Shen, N.-H., Koschny, T. & Soukoulis, C. M. Tunable terahertz meta-surface with graphene cut-wires. *ACS Photonics* **2,** 151–156 (2015).
43. Wan, W. *et al.* Time-reversed lasing and interferometric control of absorption. *Science* **331,** 889–892 (2011).
44. Zhang, J., MacDonald, K. F. & Zheludev, N. I. Controlling light-with-light without nonlinearity. *Light: Sci. Appl* **1,** e18 (2012).
45. Lin, Z. *et al.* Unidirectional invisibility induced by pt-symmetric periodic structures. *Phys. Rev. Lett* **106,** 213901 (2011).
46. Longhi, S. Pt-symmetric laser absorber. *Phys. Rev. A* **82,** 031801 (2010).
47. Hao, J., Zhou, L. & Qiu, M. Nearly total absorption of light and heat generation by plasmonic metamaterials. *Phys. Rev. B* **83,** 165107 (2011).
48. Pirruccio, G., Martín Moreno, L., Lozano, G. & Gómez Rivas, J. Coherent and broadband enhanced optical absorption in graphene. *ACS Nano* **7,** 4810–4817 (2013).
49. Sun, Y., Tan, W., Li, H., Li, J. & Chen, H. Experimental demonstration of a coherent perfect absorber with pt phase transition. *Phys. Rev. Lett.* **112,** 143903 (2014).
50. Kang, M., Chong, Y. D., Wang, H.-T., Zhu, W. & Premaratne, M. Critical route for coherent perfect absorption in a fano resonance plasmonic system. *Appl. Phys. Lett.* **105,** 131103 (2014).
51. Zheng, J., Barton, R. A. & Englund, D. Broadband coherent absorption in chirped-planar-dielectric cavities for 2dmaterial- based photovoltaics and photodetectors. *ACS Photonics* **1,** 768–774 (2014).
52. Zhang, J. *et al.* Coherent perfect absorption and transparency in a nanostructured graphene film. *Opt. Express* **22,** 12524–12532 (2014).
53. Fan, Y., Zhang, F., Zhao, Q., Wei, Z. & Li, H. Tunable terahertz coherent perfect absorption in a monolayer graphene. *Opt. Lett.* **39,** 6269–6272 (2014).
54. Wunsch, B., Stauber, T., Sols, F. & Guinea, F. Dynamical polarization of graphene at finite doping. *New J. Phys.* **8,** 318 (2006).
55. Hwang, E. H. & Das Sarma, S. Dielectric function, screening, and plasmons in two-dimensional graphene. *Phys. Rev. B* **75,** 205418 (2007).
56. Gusynin, V. P., Sharapov, S. G. & Carbotte, J. P. Magneto-optical conductivity in graphene. *J. Phys.: Condens. Matter* **19,** 026222 (2007).
57. Woessner, A. *et al.* Highly confined low-loss plasmons in graphene–boron nitride heterostructures. *Nat. Mater* **14,** 421–425 (2015).
58. Wang, L. *et al.* One-dimensional electrical contact to a two-dimensional material. *Science* **342,** 614–617 (2013).
59. Caldwell, J. D. *et al.* Sub-diffractional volume-confined polaritons in the natural hyperbolic material hexagonal boron nitride. *Nat. Commun.* **5,** 5221 (2014).
60. Tassin, P., Koschny, T. & Soukoulis, C. M. Effective material parameter retrieval for thin sheets: Theory and application to graphene, thin silver films, and single-layer metamaterials. *Physica B* **407,** 4062–4065 (2012).

Acknowledgements

Author Contributions

Y.F., Z.L. and Z.W. did the theoretical calculations and the numerical simulations. Q.F., F.Z. and Q.Z. helped the simulations. J.L., C.G. and H.L. contributed to the scientific discussion. Y.F. conceived the idea and wrote the manuscript, all authors commented on the manuscript revisions.

Additional Information

Competing financial interests: The authors declare no competing financial interests.

How to cite this article: Fan, Y. *et al.* Tunable mid-infrared coherent perfect absorption in a graphene meta-surface. *Sci. Rep.* **5**, 13956; doi: 10.1038/srep13956 (2015).